GENERAL MOTORS CORPORATION

TECHNICAL REPORT ON

MEASUREMENTS OF SHOCK WAVE PRESSURES GENERATED BY HYPERVELOCITY IMPACTS IN ALUMINUM

SPONSORED BY
NASA/MARSHALL SPACE FLIGHT CENTER
CONTRACT NO. NAS-11118

GM DEFENSE RESEARCH LABORATORIES

SANTA BARBARA, CALIFORNIA

AEROSPACE OPERATIONS DEPARTMENT

TR64-58

NOVEMBER 1964

Copy No 53

GENERAL MOTORS CORPORATION

TECHNICAL REPORT ON

MEASUREMENTS OF SHOCK WAVE PRESSURES GENERATED BY HYPERVELOCITY IMPACTS IN ALUMINUM

By Jacques A. Charest

SPONSORED BY
NASA/MARSHALL SPACE FLIGHT CENTER
CONTRACT NO. NAS-11118

GM DEFENSE RESEARCH LABORATORIES
SANTA BARBARA, CALIFORNIA

AEROSPACE OPERATIONS DEPARTMENT

TR64-58

NOVEMBER 1964

ABSTRACT

This paper presents and discusses the results of an experimental technique which has been used for determining maximum shock wave pressures generated by hypervelocity impacts of 0.476-cm aluminum spheres into 1100-0 aluminum targets. The experimental approach consists of measuring free-surface particle velocities upon arrival of shock waves at the rear surfaces of targets. Shock wave pressures were, therefore, calculated from available shock-wave data for aluminum using the approximation that free-surface particle velocity is twice the particle velocity behind the shock inside the targets. Measurements were made for various thicknesses of targets and compared with values predicted from hydrodynamic calculations. The experimental results, which were obtained at an impact velocity of 7.32 km/sec, show a very close agreement above 100 kilobars with values calculated at 7.32 and 7.62 km/sec. From the calculated and measured values of peak shock wave amplitude, the pressure is found to decay as the inverse of the 1.6-power dependence of the distance from the impact point.

CONTENTS

ILLUSTRATIONS

TABLES

INTRODUCTION

During the last few years, some investigators[1-3] have used hydrodynamic models in their analyses of hypervelocity impacts. Solutions of these theoretical approaches were obtained from Rankine-Hugoniot jump conditions across shock fronts, isentropic continuous flow equations behind shocks, and suitable equations of state of materials. However, it is not easy to verify experimentally some of these hydrodynamic treatments of hypervelocity impact phenomena. The difficulty arises from the fact that early-stage effects which are believed to be of hydrodynamic nature are obscured by the effects of the later stage of interaction when elastic plastic deformation and the strength of the material control and arrest the flow.

This paper describes an attempt to measure maximum shock-wave pressures generated by hypervelocity impacts of aluminum spherical projectiles into aluminum targets. The experimental measurements were obtained from a "Throw-off Pellet Technique" which is a version of the Hopkinson pressure-bar technique.[4] A few investigators[5,6] have used this technique for measuring amplitudes and profiles of stress waves in solids. In spite of some limitations, the "Throw-off Pellet Technique" is a very powerful tool for engineering purposes. It permits adequate measurements with limited instrumentation and calibrations.

The experimental results obtained during this series of experiments are compared with the values predicted from hydrodynamic solutions calculated with a computer code. The calculations of the computed values were based on a cylindrical projectile of volume equal to the volume of the spherical projectiles used in these experiments. It is found experimentally that projectiles having the same masses and slightly different geometrical configurations produce similar craters in semi-infinite targets. The computations of the measured pressures were made from graphical solutions.

ANALYSIS OF TECHNIQUE

Figure 1 shows the basic mechanism of the "Throw-off Pellet Technique." As has been observed in some transparent materials, a hemispherically-shaped shock wave develops in an aluminum target by the impact of an aluminum sphere. After traversing a short distance through the targets, the axial shock-wave profile is essentially the one shown on the upper part of Figure 1a, its maximum value and its wave-length being σ_M and λ respectively. If one neglects effects of rarefaction waves generated at the periphery of the pellet, which is essentially correct for thin pellets having a diameter-to-thickness ratio greater than 15, the following phenomena takes place.

As indicated in Figure 1b, the shock wave enters the pellet through the target-pellet interface without attenuation. From simple geometrical considerations, it can be shown that the portion of the shock wave which enters the pellet may be considered essentially plane if the diameter, D, of the pellet is much smaller than the distance, R, of the shock front from the point of impact. After reaching the free face of the pellet, the compression wave (+) reflects as a tension wave (-) which now moves toward the left. At the instant that the front of the tension wave reaches the

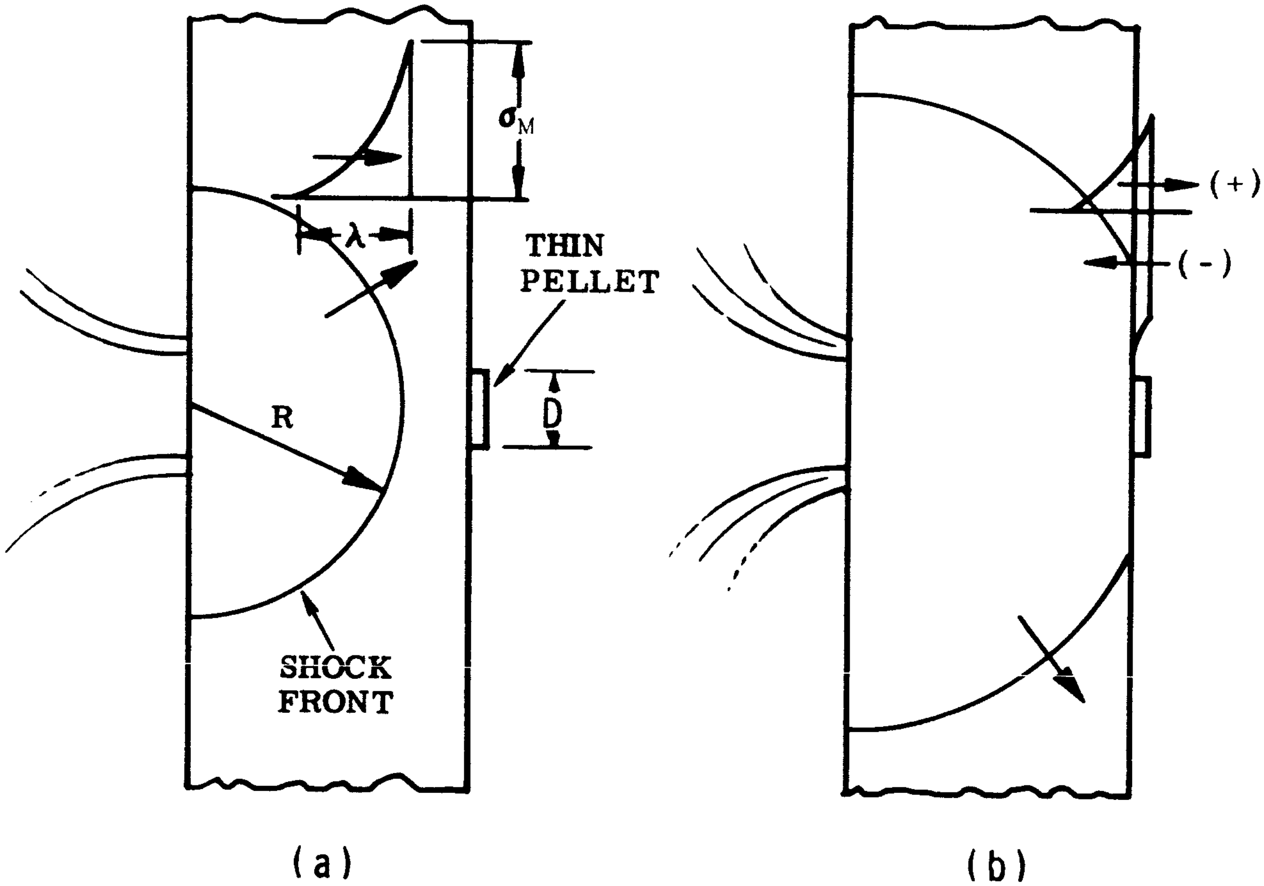

Figure 1 Fundamental Mechanism of the "Throw-Off-Pellet" Technique

target-pellet interface, the net stress at this point is therefore in tension. Since, in principle, the target-pellet interface has no strength in tension, the pellet will fly off with a velocity which is determined by the impulse transmitted to the pellet during this period of interaction.

Using Newton's second law, the amount of momentum toward the right imparted to the pellet is given by the following equation

$$\int_o^t \sigma \; A \, dt = m v_p \tag{1}$$

where σ is the stress level at any point on the shock-wave profile beyond its maximum value, A is the cross-section area of the pellet, t is the total traverse time across the pellet of the compression and tension wave, and m and v_p are, respectively, the mass and the velocity of the pellet. Using the approximation that both compression and tension waves travel through the pellet at the same velocity, U, the total traversal time, t, is therefore given by the following relation

$$t = \frac{2T}{U} \tag{2}$$

where T is the thickness of the pellet.

If the pellet is sufficiently thin, the left-hand side of Equation (1) can be rewritten and gives

$$\sigma_{av} A t = m v_p \tag{3}$$

where σ_{av} is the average stress acting on the left face pellet during time t. Inserting the value of t given by Equation (2) into Equation (3), one obtains Equation (4)

$$\sigma_{av} A \frac{2T}{U} = m v_p \tag{4}$$

Since the mass of the pellet is equal to ρ A T and the stress can be expressed by the well-known relationship $\sigma = \rho U \mu$, where μ is the particle velocity behind the shock front in the target or in the pellet, one obtains

$$\rho U \mu_{av} \cdot \frac{A\ 2T}{U} = \rho A T v_p \tag{5}$$

or

$$2 \mu_{av} = v_p \tag{6}$$

Equation (6) expresses the fact that the flying velocity of the thin pellet is twice the average particle velocity of the shock-wave portion captured by the pellet during the time of interaction. In other words, if the pellet is sufficiently thin, it will move at about the same maximum velocity as the free rear surface of the target upon arrival of the shock.

EXPERIMENTAL APPROACH

Figures 2a, 2b, and 2c illustrate the experimental technique which has been used for measuring shock-wave pressures generated by hypervelocity impacts of aluminum spheres into aluminum targets. As seen in Figure 2, the technique consisted of impacting a target at a given point and observing the motion of a thin pellet which had been previously affixed on the rear surface of the target immediately behind the point of impact. Upon arrival of the shock wave at the rear surface of the target, the pellet flies off and its velocity is measured using high-speed photography techniques. The aluminum projectiles (0.76-cm spheres) were accelerated to about 7.32 km/sec using a split-sabot technique and a 7.61-mm-bore, constant-base-pressure light-gas gun. The impact velocities were measured to within 1% deviation using a combination of photo-beam detectors and shadowgraph systems.

A Beckman and Whitley framing camera (Model 192) was used to record the motion of the thin pellets. A high-intensity and controlled-duration light source was triggered a few microseconds before impact and a beam of parallel light was obtained at right angle to the field of interest and directed toward the camera by means of a Fresnel lens.

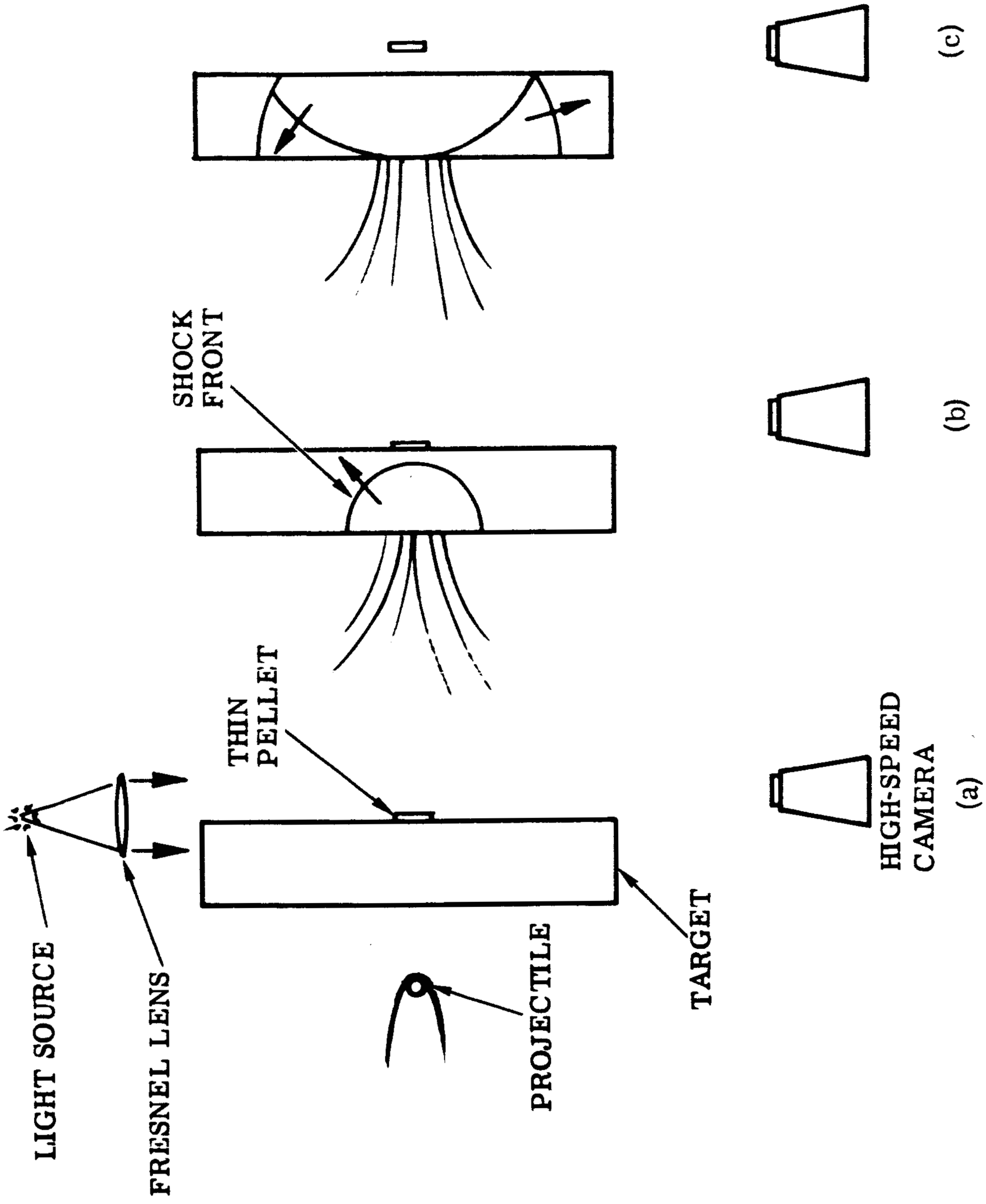

Figure 2 Sequence of Events Illustrating the "Throw-Off-Pellet" Technique

In order to avoid mismatch problems at the interface of the target-pellet, the thin pellets were also made of 1100-0 aluminum; their diameters and thicknesses were respectively 6.35 mm and 0.40 mm. The thicknesses of the targets were varied from 1.1 to 8.0 cm and their side dimensions were held constant at 10 cm.

The tests were conducted at a range pressure of about 30 mm of Hg, using the hypervelocity impact facilities at GM Defense Research Laboratories. The "Throw-off Pellet Technique," such as seen in Figure 2, was used for measuring pressures below 100 kilobars. For higher pressure, the technique consisted of observing the maximum velocity at the front of the bubble of debris behind the targets. This modified technique, which is essentially the same as the "Throw-off Pellet Technique," was used for thicknesses of targets smaller than 1.10 cm.

EXPERIMENTAL RESULTS

Table I shows the values of maximum shock wave pressures predicted from hydrodynamic solutions. Table II contains the experimental data which have been collected during this series of tests. The calculated pressure values were obtained from two different sources.[3,7] Heyda's and Riney's values were obtained at 7.62 km/sec of impact velocity, V_o, using a flat cylindrical projectile having a diameter-to-height ratio equal to two. Tillotson's values were obtained at 7.32 km/sec of impact velocity and a more realistic projectile of diameter-to-height ratio equal to one. In both cases, the volumes of the projectiles were equal to the volume of the spheres used for the experiments.

In order to determine from experiments the maximum shock-wave pressures generated by impacts of the projectiles, a plot was obtained from available literature[8,9] showing pressures versus particle velocities behind shocks in aluminum. This plot is shown in Figure 3. Using the free surface particle velocities, such as measured by the experiments, and converting to particle velocities behind the shock in the material, it is therefore possible to obtain Figure 4 from Figure 3. Figure 4, which shows the maximum shock-wave pressures versus distances from points of impact, is based on the assumption that the free surface particle

Table I. Calculated Maximum Shock-Wave Pressures Generated by Impacts of Flat Cylindrical Projectiles Into Aluminum Targets

Heyda's and Riney's Solution 0.262 cm = h 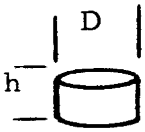 D/h = 2 V_o = 1.62 km/sec		Tillotson's Solution 0.420 cm = h 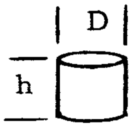 D/h = 1 V_o = 7.32 km/sec	
DISTANCE cm	PRESSURE Kbars	DISTANCE cm	PRESSURE Kbars
0.31	1,147	0.32	1,000
0.35	1,110	0.38	700
0.37	736	0.45	500
0.41	600	0.53	380
0.49	473	0.67	250
0.62	443	0.78	200
0.75	202		
0.78	223		
0.85	224		
0.92	211		
1.11	107		

Table II. Experimental Data Used for Determining Maximum Shock-Wave Pressure Generated by Impact of 0.476-cm Aluminum Spheres Into Aluminum Targets at 7.32 km/sec

TARGET THICKNESS cm	IMPACT VELOCITY km/sec	FREE SURFACE PARTICLE VELOCITY km/sec	MEASURED PRESSURE Kbars
0.51	7.41	3.300	352.0
0.76	7.11	2.170	206.0
1.02	7.26	1.622	150.0
1.02	7.33	1.431	130.0
1.53	7.26	0.894	78.6
1.91	7.39	0.590	49.6
2.54	7.20	0.372	31.5
3.05	7.36	0.283	23.9
3.55	7.41	0.245	19.8
4.80	7.62	0.160	12.0
6.40	7.62	0.093	7.6
7.61	7.03	0.040	5.3

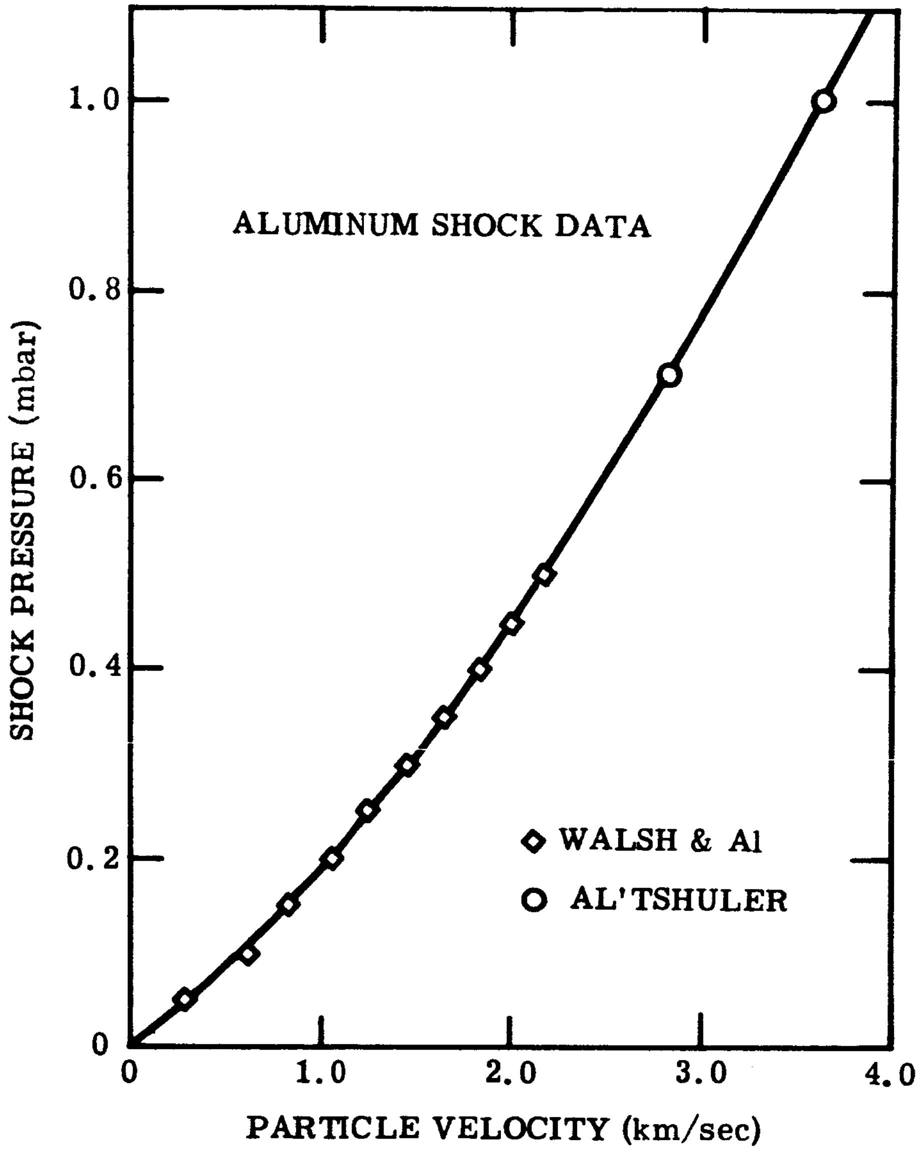

Figure 3 Shock-Wave Pressure vs Particle Velocity in Aluminum

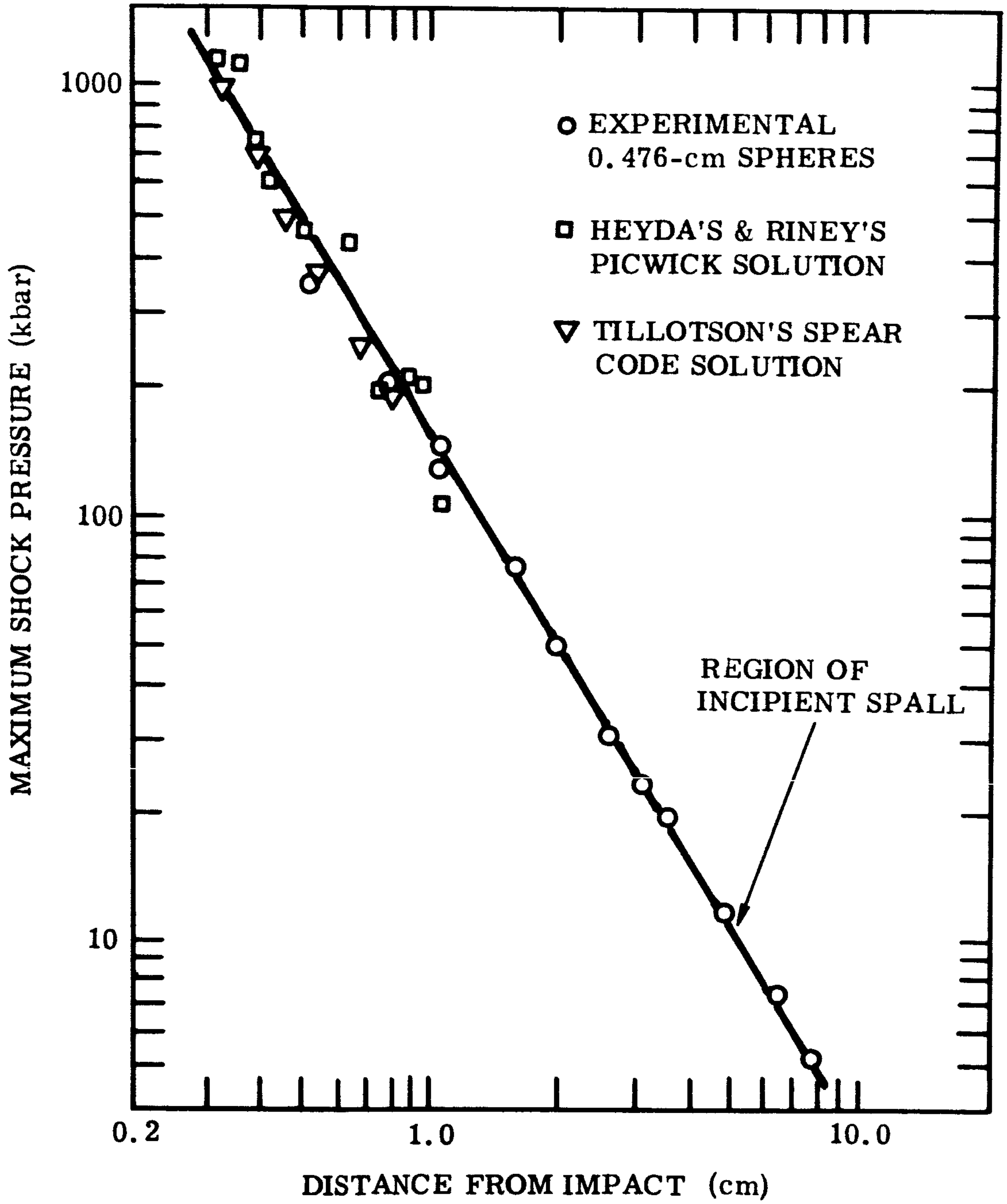

Figure 4 Calculated and Measured Maximum Shock-Wave Pressures Generated by Impacts of Equivolume Projectiles into 1100-0 Aluminum Targets

velocity is twice the particle velocity behind the shock in the material. The maximum error induced in the calculations using this assumption was estimated to be 3% at 500 kilobars.[10] The predicted values of pressures given in Table I are also presented in Figure 4 for purpose of comparison.

During this series of tests, the thickness of one of the targets was adjusted so that incipient spall could be observed near its rear face. The thickness was calculated from previous experiments involving measurements of the incipient spall threshold of 1100-0 aluminum at stress level zero. Using impacts of flat plates, this value was found to be about 10.7 kbars. As shown in Figure 4, it was found that a 5.0 cm target should show an incipient spall close to its rear face if impacted at about 7.32 km/sec with a 0.476-cm aluminum sphere. A special target was, therefore, made for such observation and its configuration is shown at real scale in Figure 5. As predicted, an incipient spall was found at about 4 mm from the rear face of the target. As shown in Figure 5, this special target served also to measure simultaneously the shock-wave pressure at two distances from the point of impact. From the spall thickness, it has also been possible to estimate the wavelength of the shock wave at 5.0 cm away from the point of impact. Since in the case of incipient spall the maximum amplitude of the shock wave has the same values as the critical stress of the material, the wavelength is therefore twice the spall thickness of 8 mm for this particular case.

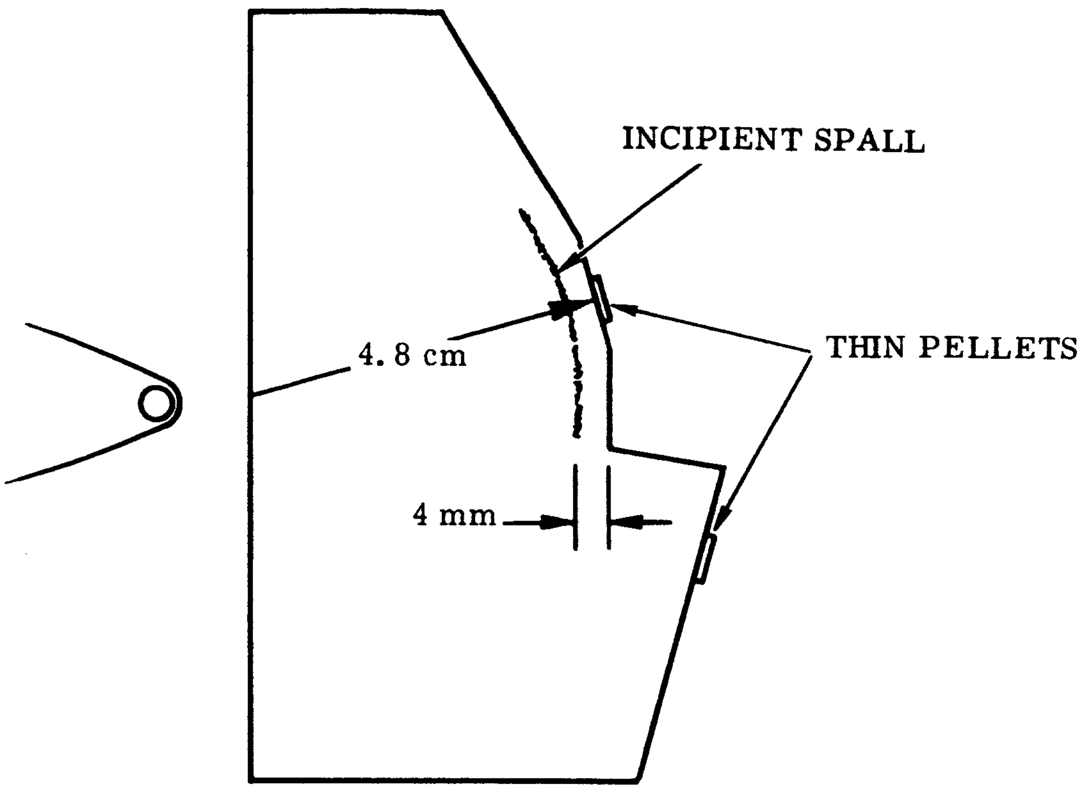

Figure 5 Special Target Used for Observing Incipient Spall

DISCUSSION

From Figure 4 it is possible to obtain an engineering relationship giving the maximum shock-wave pressure in 1100-0 aluminum as a function of distance from impact. If a straight line is fitted through the calculated and experimental results, the following equation is obtained

$$\sigma_M = 1.234 \ \sigma_H/(R/R_o)^{1.6} \quad R > 1.14 \ R_o \tag{7}$$

where σ_H is the Hugoniot pressure at corresponding impact velocity and R_o is the effective radius of the projectile. The 1.6-distance power dependence of Equation (7) applies more specifically to pressures below 0.3 megabar, since the calculated values indicate a 1.8-distance power dependence for pressure between 0.3 and 1.0 megabar.

The lower limit, 1.14 R_o, of Equation (7) was obtained by extrapolating the curve of Figure 4 to the Hugoniot maximum pressure at 7.32 km/sec impact velocity. In the case of a flat cylindrical projectile of radius R_o, it was found experimentally[11] that the rarefaction waves generated at the edges of the projectile catch up with the compression wave at a distance of about 1.4 R_o along the axis of symmetry in the target. The lower limit, 1.14 R_o, found in this work is explained by the rarefaction waves which are generated at points closer to the axis of symmetry. These, in turn, make the compression wave decay at a lesser distance in the target than in the case of a flat cylindrical projectile.

Equation (7) has been derived only from the results presented in this paper and could be slightly different in predicting pressure with materials and projectiles other than the ones used here. However, until more experimental results become available, shock wave pressure in soft aluminum can be learned from Equation (7) for projectiles having comparable diameters to 0.476-cm spheres. This last statement is justified by the scaling law which is found to hold in theoretical calculation.

CONCLUSION

The good agreement between the calculated and the measured shock-wave pressures shown in Figure 4 is very significant. It strongly indicates that the hydrodynamic model assumed for the calculations was suitable for the present case. Also, the "Throw-off Pellet Technique" has been shown to be a promising technique for measuring shock-wave pressures. Since there exists a unique relation between shock pressure particle velocities, shock velocities, and densities of material, it is therefore possible to determine any of them once particle velocity is known. It is therefore possible to evaluate to great accuracy the arrival time of shock waves after impact.

REFERENCES

1. R. L. Bjork, Tenth International Astronautical Congress, London, 505, 1959

2. J. M. Walsh and J. H. Tillotson, Proceedings of the Sixth Symposium on Hypervelocity Impact, Vol. II, Part 1, 59

3. J. F. Heyda and T. D. Riney, "Penetration of Structures by Hypervelocity Projectiles," Space Science Laboratory, General Electric Company

4. B. Hopkinson, Trans. Roy. Soc., London, A 213, 437, 1914

5. J. S. Rinehart, J. Appl. Phys., 22, 555, 1951

6. J. L. O'Brien, Office of Naval Research, NONR 1866 (35) 1961

7. J. H. Tillotson, Private Communication, GM Defense Research Laboratories, Santa Barbara, California

8. J. M. Walsh, et al, Phys. Rev., 108, 196, 1957

9. L. V. Al'Tshuler, et al, Soviet Physics, JETP, 11, 573, 1960

10. M. H. Rice, R. G. McQueen and J. M. Walsh, Solid State Physics, 6, Academic Press, Inc., New York, 1958

11. L. V. Al'Tshuler, et al, Soviet Physics, JETP, 38, 1061, 1960

ACKNOWLEDGMENT

The author wishes to thank J. H. Tillotson and A. H. Jones for their constructive criticisms made in respect to this work. He also wishes to thank NASA/Marshall Space Flight Center for permitting the release of the content of this work.